Simulating CW Light Propagation Through Macroscopic Scattering Media Via Optical Phase Conjugation

Yi-An Huang, Cheng-Hao Tsai, and Snow H. Tseng*

Graduate Institute of Photonics and Optoelectronics
National Taiwan University, Taipei, 10617 Taiwan
r98941072@ntu.edu.tw, r98941072@ntu.edu.tw, stseng@ntu.edu.tw*

Abstract **─** The pseudospectral time-domain (PSTD) technique is advantageous for modeling macroscopic light scattering problems but falls short to model a light source of realistic dimensions. We report a novel simulation technique that enables modeling a finite-width, continuous-wave (CW) light source within PSTD simulations that was infeasible before. By exploiting the mathematical characteristics of Maxwell's equations, the instability problem of the PSTD algorithm can be overcome. We demonstrate the reported simulation enables modeling the CW optical phase conjugation (OPC) phenomenon of light propagation through a scattering medium. Specific simulation findings show that monochromatic phase-conjugated light can be focused through scattering medium. On a wider scope, the reported method enables implementing a finite-width, CW, plane-wave light source in a PSTD simulation for general optics and electromagnetic problems.

Index Terms **─** CW, Maxwell's equations, multiple scattering, optical phase conjugation, PSTD, simulation.

I. INTRODUCTION

Biomedical optical techniques are generally limited to surface applications due to the limited penetration depth of optical wavelengths. If optical wavelengths can penetrate deeper through biological tissue structures, the applicability of biomedical optics can be extended beyond the surface. In 2007, Lerosey et al. reported experimentally demonstrating delivering electromagnetic wave beyond the diffraction limit by means of random metallic scatterers [1]. Recently, much research effort to enhance the penetration depth of visible light through turbid media has been reported [2-4]. Utilization of the optical phase conjugation (OPC) phenomenon has been reported to enhance light penetration through turbid media (e.g., biological tissue) by canceling out the incoherent light scattering effect that causes opacity [5]. The OPC phenomenon causes multiply scattered light to propagate in reversed directions, retrace its previous scattering trajectory, and essentially penetrate through turbid media. Initial experimental effort was done by utilizing a nonlinear crystal [5]; later, a digital optical phase conjugation technique using an optical wavefront sensor and spatial light modulator was reported that significantly enhances the performance, speed, and flexibility of light penetration [6]. Due to the extreme complexity involved for light propagation through macroscopic random media, such phenomena are difficult to analyze. An accurate simulation technique based upon the Maxwell's equations that can account for the wave characteristics of light is desired.

Based upon numerical solutions of Maxwell's equations, the pseudospectral time-domain (PSTD) technique is computational economic and can model macroscopic light scattering problems [7] that the finite-difference time-domain (FDTD) technique falls short. However, due to the Fourier transforms involved, the conventional PSTD algorithm is incompatible with field discontinuities therefore cannot model a light source of realistic dimensions; typically in a PSTD simulation the light source is modeled by a plane wave with infinite extent. In this manuscript, we report a novel simulation technique that enables modeling a CW plane wave light source of arbitrary width within a PSTD simulation for the first time. The CW OPC simulation consists of two parts: the modeling of *forward propagation* and the modeling of *backward propagation*. In Section III (*forward propagation*): the implementation of a finite-width, CW light source is explained in detail. The key to successfully implementing a finite-width, plane-wave illumination is discussed. In Section IV (*backward propagation*): simulating the reversed propagation of CW OPC phenomenon is described. Together, the *forward propagation* and *backward propagation* enable robust modeling of the CW OPC phenomenon of light penetration through large-scale turbid media (e.g., biological tissues structures).

II. PSEUDOSPECTRAL TIME-DOMAIN ALGORITHM

To model the OPC phenomenon, the PSTD

Submitted On: January 4, 2015
Accepted On: February 21, 2016

algorithm [7] is employed to obtain numerical solutions of Maxwell's equations. The PSTD algorithm is advantageous for large-scale electromagnetic wave propagation problem. In the PSTD algorithm, temporal derivatives of Maxwell's equations are calculated using a 2nd-order central difference scheme, whereas the spatial derivatives are evaluated by forward and inverse Fourier transforms:

$$\left\{ \frac{\partial E}{\partial x}\bigg|_i \right\} = -F^{-1}\{jk_x \cdot F\{E_i\}\}, \quad (1)$$

E is the electric vector field, k_x is the wave number, and **F** represents the Fourier transform. Since computer calculations are based on discrete numbers, discretization of the continuous electromagnetic fields is necessary. According to the Nyquist sampling theorem, the spatial derivatives calculated in Eq. (1) is of spectral accuracy (meaning as accurate as it can get with the given information), allowing the PSTD technique, with a coarse grid of two spatial samples per wavelength, to achieve similar accuracy as the finite-difference time-domain (FDTD) technique (FDTD requires 20 spatial samples per wavelength.) The coarse spatial grid points enables simulating the large-scale optical phenomena with economic computational memory; for example, to simulate a 3-D light scattering problem with the same computational memory, the PSTD technique can model up to approximately 1000-time larger light scattering problem than the FDTD technique. Finally, the anisotropic perfectly matched layer (APML) absorbing boundary condition [8] is implemented to absorb all outgoing waves. If all outgoing waves never re-interact with the medium, the optical simulation can be considered as being practically isolated in vacuum.

III. FORWARD PROPAGATION

Biomedical optics typically involve a macroscopic scattering medium illuminated by a finite-width, CW light source; thus, a simulation technique capable of modeling a finite-extent illumination in a large-scale light scattering problem is needed. The FDTD simulation of light propagation through small-scale turbid media has been reported [9]; however, the employed hard source [10] generates artificial scattering that causes inevitable error to the simulation. The PSTD algorithm is computationally memory-efficient and can model larger problems; simulation of the pulse OPC phenomenon using the PSTD algorithm has been reported [11]. However, previous reported simulation technique falls short to model the CW OPC phenomenon that is more realistic for most optical techniques. Furthermore, due to the Fourier transforms involved, the widely used total-field/scattered-field (TF/SF) formulation [10] for FDTD simulations is not compatible with the PSTD algorithm; also, the PSTD algorithm cannot handle a point light source [12]. As a result, a CW light source of realistic size that is stable in a large-scale PSTD light scattering simulation was not feasible, seriously hindering the applicability of the PSTD technique to model practical problems. A finite-width, CW light source compatible with the PSTD algorithm is required.

By exploiting the mathematical characteristics of Maxwell's equations, we report a novel method to implement an arbitrary CW light source that is stable in the PSTD simulation. A flow chart of the PSTD algorithm is shown in Fig. 2. The characteristics of Maxwell's equations are such that the electromagnetic fields depend on the changes of local electromagnetic fields rather than remote electromagnetic fields. Therefore, the numerical artifacts caused by field discontinuities are most pronounced in its vicinity; the effect of field discontinuities far away is limited as it decreases inversely with distance squared. A locally continuous electromagnetic field suffices for the PSTD algorithm to update the local electromagnetic field. To model a CW light source within the simulation space, the electromagnetic field of a finite-width, sinusoidal CW plane-wave is added into the *source region* at each time-step:

$$E_i = e^{-\left(\frac{y-y_0}{\sigma_y}\right)^2} \cos[k(x-x_0)-\omega t], \quad (2)$$

(x_0, y_0) is the center of the light source, whereas width and thickness denote the *x*-dimension and *y*-dimension of the *source region*, respectively (as shown in Fig. 1). To prevent artificial scattering from the *source region*, the inserted optical field is added into space as a "soft source" [13]. A Gaussian profile (Eq. (2)) is employed in the *y*-direction to smooth out field discontinuities of the finite-width plane wave.

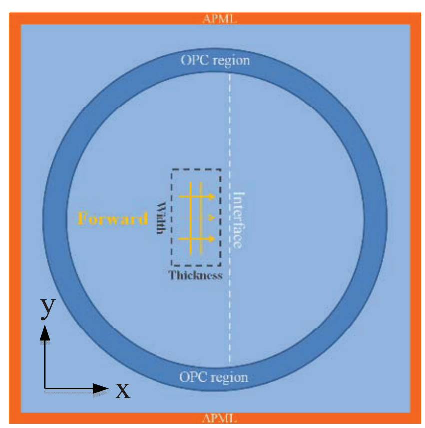

Fig. 1. Schematics of simulating a finite-width, CW plane wave light source in a PSTD simulation. A CW plane wave superimposed into the simulation space in the source region (the dashed rectangular region).

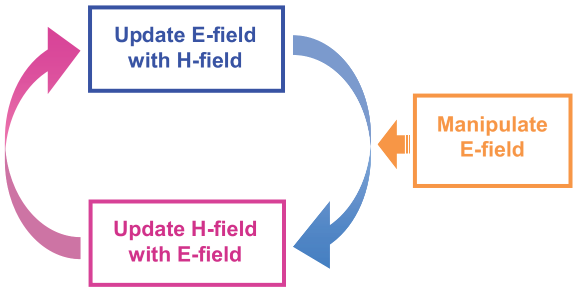

Fig. 2. Flow chart of PSTD algorithm of modeling CWOPC phenomenon. The ***E***-field and ***H***-field are updated consequently from each other. As the ***E***- and ***H***-fields are updated based upon Maxwell's equations, manipulation of the fields is performed to generate the desired light source.

Instead of a point light source in the PSTD simulation, the incident light is introduced into the simulation space as a piecewise continuous segment of electromagnetic fields (e.g., 5-µm-by-10-µm patch of smooth electromagnetic field), as shown in Fig. 3 (a). The piecewise continuous segment of field ensures stability of the PSTD algorithm, thus, the electromagnetic fields inside or outside the source region is stable and can be updated correctly with light propagating in the forward direction (Fig. 3 (b)). Initially, as the incident field is initially added into the simulation space, transient numerical artifacts of high-frequency oscillation emerge due to the abrupt discontinuity of the electromagnetic fields. Without the constant amplitude of an infinite plane wave in *x*- and *y*-directions, edges of the finite-width plane wave deteriorates (Figs. 3 (c) and 3 (d)). With support from the finite-width CW plane wave continuously added into the source region, the incident plane wave continues to propagate in the forward direction while maintaining its width *w* (Fig. 3 (e)). As the emitted light reaches steady state, instability at the edges disappears leaving only a finite-width, CW plane wave propagating steadily in the forward direction within the PSTD simulation (Fig. 4).

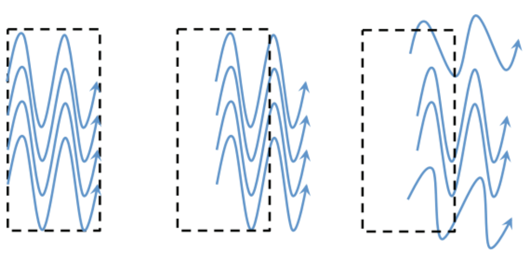

(a) (b) (c)

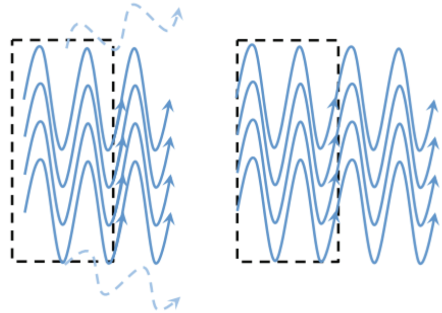

(d) (e)

Fig. 3. Schematics of implementing a finite-width CW plane wave light source in the PSTD simulation. (a) A plane wave with a cross-sectional width *w* is added into the *source region* (dashed box). (b) As time evolve, light propagates in the forward direction. (c) Without the neighboring field of an infinite plane wave, edges of the finite-width plane wave deteriorate. (d) Incident field is added into the *source region* in the next time-step. Supported by the incident finite-width plane wave continuously added into the *source region*, the field continues to propagate in the forward direction steadily.

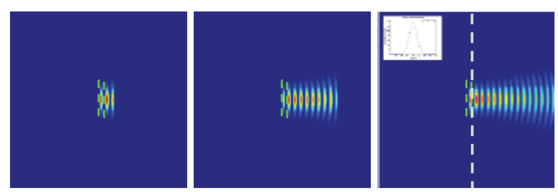

(a) (b) (c)

Fig. 4. (Media 1) A stable light source emitting a CW, finite-width, plane wave in a PSTD simulation. (a) Sinusoidal electromagnetic field added into space at the *source region* (the green dashed rectangular region). (b) Later inserted electromagnetic field propagates and connects with the previously inserted electromagnetic field. (c) Once the steady state is reached, the sequentially inserted electromagnetic fields together form a CW, finite-width propagating plane wave. The CW cross-sectional amplitude profile of the light beam is shown in the inset-figure (as measured along the white dashed line in Fig. 1).

Width of the *source region* determines the cross-sectional extent of the emerging CW light, whereas the amplitude of the CW light is proportional to the thickness of the *source region*. For instance, the amplitude E_{zo} of the sinusoidal plane wave $E_{zi} = A \cdot sin(kx - \omega t)$ emitted from the *source region* as is given by:

$$E_{zo} = \frac{m \cdot \Delta x}{c \cdot \Delta t} E_{zi}, \quad (3)$$

where m is the number of grid layers of the *source region*, Δx and Δt are the spatial and temporal grid spacing, respectively, and c is the speed of light. Incident light as a patch of continuous field of the *source region* is added into the simulation; this minimizes the numerical artifacts to maintain numerical stability. The field added into the simulation is proportional to the area of the *source region*, therefore, amplitude of the incident light is proportional to the *thickness* ($m \cdot \Delta x$) of the *source region*. Light generated from this CW light source propagates in the direction of the Poynting vector. For a typical OPC simulation of light propagation through turbid medium, the turbid medium is illuminated by the incident CW light, where light scatters into various directions. Once the steady state is reached, the outward propagating CW light is recorded in the *OPC region* (as shown in Fig. 1), which is later used in modeling *backward propagation* of phase-conjugated light, as discussed in Section IV.

Simulation artifacts caused by discontinuity of the electromagnetic field must be minimized to maintain numerical stability. The *source region* is smooth and continuous both in the *x*- and *y*-directions with minute discontinuities at the edges. For a finite-width plane wave, the discontinuity at the edges of the *source region* causes numerical artifacts. It is critical that the source region be wide and smooth enough in both *x*- and *y*-directions; if the *source region* is too narrow, numerical artifacts emerge due to the Gibbs' phenomenon. By increasing the piecewise continuity of the field in the *source region* and its neighborhood, the numerical artifacts are reduced. Or, smoothening the inserted electromagnetic field with a Gaussian profile can also significantly reduce the high-frequency numerical artifacts. If the overall electromagnetic field only consists of a small fraction of the electromagnetic field that is discontinuous, the simulation artifacts are localized and decay as the CW steady state is reached. Convergence analyses show that error decreases rapidly as the *source region* becomes thicker than a few grid points.

The proposed light source implementation enables creating a CW, plane-wave light source of arbitrary width. The amplitude of light emitted from the proposed light source in vacuum is shown in Fig. 5 (a). The amplitude profiles of a CW plane wave is measured adjacent to the *source region.* Due to diffraction of light, the amplitude profile is not constant but varies in space; for a plane wave with a larger cross-section, the profile becomes constant with undulation at the edge of the plane wave. The amplitude of light emitted from the proposed light source embedded in a scattering medium is shown in Fig. 5 (b); the scattering medium consists of 800 6-μm-diameter, dielectric (n = 1.2) cylinders clustered in a region of 180-μm-radius. Light reflected and refracted from the scattering medium interferes with light emitted from the CW light source; the superposition of all these light components result in a complex amplitude profiles of Fig. 5 (b). As demonstrated in Fig. 5, a CW light source with realistic dimensions can be implemented without instablizing the PSTD simulation; the proposed simulation technique enables PSTD modeling a CW, finite-width, plane-wave light source embedded inside a macroscopic scattering medium.

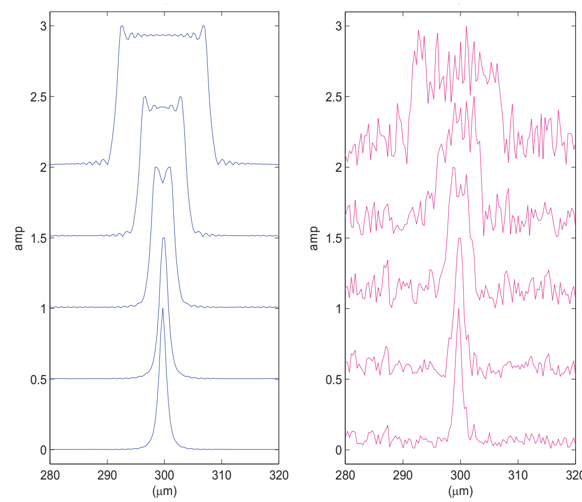

Fig. 5. (a) Implementation of a CW light source of various widths (w) in vacuum. (b) Implementation of a CW light source of various widths (w) embedded in a scattering medium (from bottom to top) w = 1, 2, 4, 8, and 16 μm, respectively. The scattering medium consists of 800 6-μm-diameter, dielectric (n = 1.2) cylinders clustered in a region of 180-μm-radius. The amplitude profile (measured along the white dashed line of Fig. 1) is more complex due to interference of light reflected and refracted from the scattering medium.

IV. BACKWARD PROPAGATION

In modeling the *backward propagation*, the OPC reversed propagation of light is generated with the CW amplitude and phase previously recorded in the f*orward propagation*. Similar to the *forward propagation*, the phase-conjugated electromagnetic field is added into the *OPC region* (Fig. 6) as a soft source [13]. Having the OPC region implemented as a soft source eliminates the artificial reflection from the *OPC region.* After the simulation reaches steady state, the temporal variation of the electromagnetic field becomes periodic: the electromagnetic field at everywhere oscillates with the same frequency throughout the entire simulation space.

In the *forward propagation*, the electromagnetic field in the *OPC region* is recorded and the CW amplitude and phase are calculated via Fourier transform. In the *backward propagation*, the phase-conjugated CW steady-state sinusoidal electromagnetic field is added into the *OPC region* to generate the reversed propagation of phase-conjugated light. The added field emerging at the *OPC region* essentially serves as the "light source" in the *backward propagation*. Simulation artifacts occur as the initially added electromagnetic fields caused by the abrupt variations at the boundary of the *OPC region*. The discontinuities at the edges excite high-frequency numerical artifacts; as the CW electromagnetic field is continuously added into the *OPC region*, numerical artifacts gradually decay, leaving only the steady-state, phase-conjugated light propagating in reversed directions.

In Fig. 7, a simulation of phase-conjugated, CW light propagation is depicted. The scattering medium consists of 1600 6-μm-diameter, dielectric (n = 1.2) cylinders clustered in a region of 180-μm-radius. Initially, phase-conjugated light (λ = 8 μm) is added into space at the ring-shaped *OPC region* (Fig. 6). The phase-conjugated light is continuously added into the ring-shaped *OPC region* and merges with the neighboring field to form a smooth, CW phase-conjugated light propagating through the scattering medium as shown in Figs. 7 (b,c). The CW, monochromatic, phase-conjugated light of wavelength λ back-propagates through the scattering medium and reconstructs the original emitted light profile (Fig. 8).

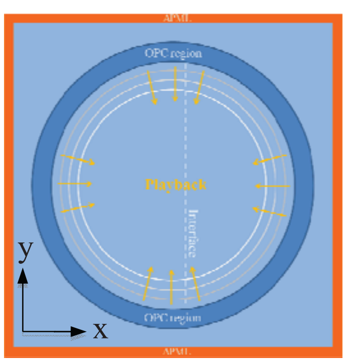

Fig. 6. CW light recorded in the *forward propagation* is phase-conjugated and added into the *OPC region* (the blue shaded region) as a soft source.

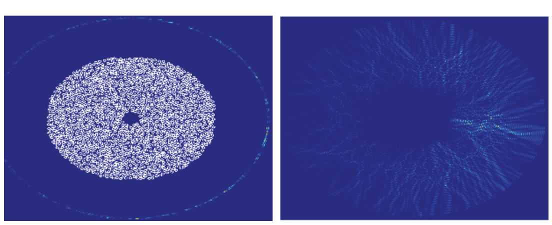

(a) (b)

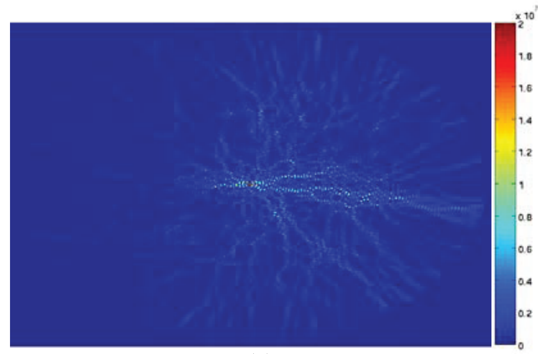

(c)

Fig. 7. (Media 2) Modeling the *backward propagation* of phase-conjugated light through scattering medium. (a) Phase-conjugated light (λ = 8 μm) is added into space at the ring-shaped *OPC region* and converges upon a scattering medium consisting of 1600 6-μm-diameter, dielectric (n = 1.2) cylinders clustered in a region of 180- μm-radius. (b) Phase-conjugated light is continuously added into space at the ring-shaped *OPC region*, and merges with the previously added field. (c) The electromagnetic field merges to form a smooth, CW phase-conjugated light propagating through the scattering medium towards its center as the simulation reaches steady state.

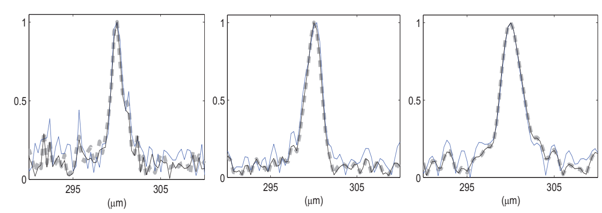

(a) (b) (c)

Fig. 8. Simulating phase-conjugated light back-propagating through a scattering medium to a narrow peak. The scattering medium consists of 1600 randomly positioned, 6-μm-diameter dielectric (n = 1.2) cylinders. A 4-μm-wide plane-wave light source (wavelength λ) is embedded at the center of the scattering medium. From top to bottom: (a) λ = 1 μm, (b) λ = 2 μm, (c) λ = 3 μm, respectively. In each subplot, the forward propagation light profile (gray dashed line) is compared to the back-propagated light (blue line) and the back-propagated light with a soft sink to eliminate the outgoing light component (black solid line).

The field discontinuity is minimized by continuously adding field at the *OPC region* which maintains numerical stability of the PSTD simulation. The CW phase-conjugated light is added into space in the *OPC region* at every time-step. For the same reason as the CW light source described in Section II, a wide and smooth enough of electromagnetic field at the *OPC* *region* is required to avoid numerical artifacts. A convergence analysis is shown in Fig. 9. Various factors affect the convergence, mainly related to the geometry such as refractive index distribution, size of the scattering medium, optical wavelength of incident light, complexity of the scattering medium, etc. Generally larger scattering medium or more complex geometry would require longer run-time to converge. For the reported simulations, an *OPC region* with a thickness of ~10 layers is sufficient to minimize numerical artifacts.

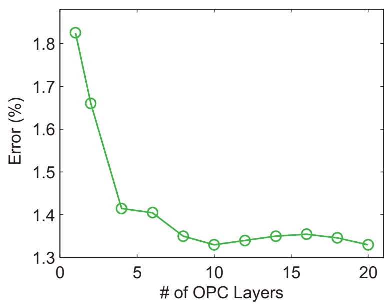

Fig. 9. Convergence analysis for the numbers of layers of the *OPC region.* The errors are evaluated by calculating the normalized, root-mean-square error between the forward outgoing and playback incoming cross-sectional profiles of the E-field. As the layers of the *OPC region* is increased, the error rapidly decreases. A 10-layer *OPC region* is sufficient to insure numerical stability.

V. DISCUSISONS

PSTD algorithm is vulnerable to discontinuities; by adding piecewise continuous electromagnetic fields, instabilities of the PSTD algorithm can be avoided. A finite-width, CW light source of arbitrary width *inside* a PSTD simulation can be modeled with the proposed simulation technique. The number of layers of the *OPC region* has to be large enough to ensure piecewise continuity. The performance of the proposed method can be evaluated by comparing the outgoing wave and the incoming wave in the *forward propagation* and *backward propagation*, respectively. If the proposed method works properly, the outgoing field would match the incoming field as in time reversal. To quantitatively evaluate the performance, the error is evaluated by calculating the normalized root-mean-square error of the *E*-field of the incoming and outgoing wave along an arbitrary cut:

$$Error_{RMS} = \sqrt{\frac{\sum_{i=1}^{n}\left[E_{Playback}(i) - E_{Forward}(i)\right]^2}{n}}, \quad (4)$$

where $E_{Forward}$ and $E_{Playback}$ are the E-field amplitude recorded along the selected cut (as shown in Figs. 1 and 6, respectively). Based upon the uniqueness theorem, the electromagnetic field along an arbitrary cut matches only if the forward propagation and backward propagation are both modeled accurately. In Fig. 9, we demonstrate that as the number of layers of the OPC region increases beyond a threshold, the error is minimized. A minimal number of layers of the source region and OPC region are required to maintain numerical stability. In order to generate an undistorted backward propagating field, the OPC region has to match the wavefront morphology. This requirement can be met when the light is scattered into all directions by a random medium, and the OPC region is far enough whereas outgoing light mostly impinges the OPC region normally. The amplitude of the simulation has to be properly scaled (Eq. 3) to satisfy energy conservation where the number of layers is proportional to the amount of light “added” in to the simulation space.

The forward and backward propagation of light through a scattering medium is simulated using the proposed simulation technique. A finite-width, CW, plane-wave light source is embedded inside a scattering medium; the scattering medium consists of 1600 randomly-positioned, 6-μm-diameter dielectric (n = 1.2) cylinders within a round region with an overall diameter of 360 μm. Various widths of the CW light source are modeled. Due to interference of scattered light caused by the scattering medium, a complex amplitude profile is recorded. The simulation technique reported in this manuscript makes it possible, for the first time, to accurately simulate the CW OPC phenomenon of a light propagation through macroscopic turbid media (e.g., biological tissues) using the PSTD algorithm [14]. As shown in Fig. 10, the OPC backward propagation of a 4-μm-wide, CW light source illuminating a 1000-μm-by-1000-μm turbid medium consisting of 670 biological cells is simulated using 12 Intel CPUs that took ~48 hours. Recently, a two-dimensional (2-D) FDTD simulation analysis of phase-conjugated light propagation through scattering medium has been reported [9]. Due to the limitations of the FDTD technique, a smaller geometry of 60-μm-by-100-μm was modeled. Another simulation analysis has been reported by Carminati et al. [2] where a scattering medium (cylindrical region of radius R = 1.91 μm) is modeled by a cluster of *idealized point dipoles*. Instead of treating each scatterer as an idealized point dipole, we model the scattering medium via a grid-based PSTD simulation. To date, the reported simulation technique is the only method that can model such large-scale CW OPC phenomenon based upon numerical solutions of Maxwell’s equations.

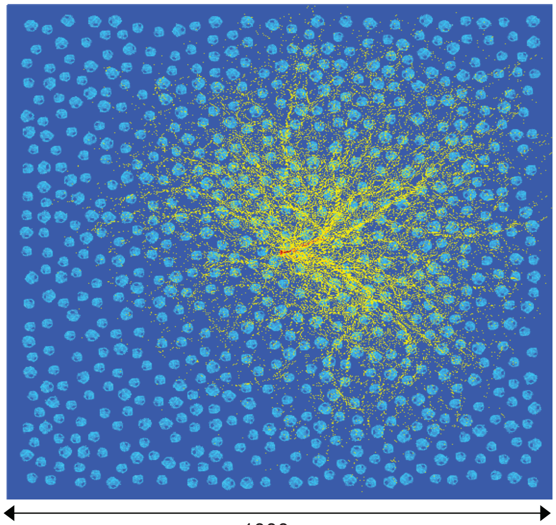

Fig. 10. CW OPC simulation of light propagating through a biological turbid medium. Light illuminating a 1000-μm-by-1000-μm tissue consisting of 670 randomly positioned biological cells is simulated. The diameter of each biological cell is approximately 20-30 μm. The illumination electromagnetic wavelength λ = 4 μm with a cross-sectional width of 10 μm.

ACKNOWLEDGMENT

This research is supported by the Taiwan National Science Council Grant NSC 99-2112-M-002-016-MY3, NSC 102-2112-M-002-020 and NSC 102-2628-M-002-006-MY3. The authors thank Changhuei Yang and Meng Cui for insightful discussions.

REFERENCES

[1] G. Lerosey, J. De Rosny, A. Tourin, and M. Fink, "Focusing beyond the diffraction limit with far-field time reversal," *Science*, vol. 315, pp. 1120-1122, 2007.

[2] R. Pierrat, C. Vandenbem, M. Fink, and R. Carminati, "Subwavelength focusing inside an open disordered medium by time reversal at a single point antenna," *Physical Review A*, vol. 87, 041801(R), 2013.

[3] J.-H. Park, C. Park, H. Yu, J. Park, S. Han, J. Shin, S. H. Ko, K. T. Nam, Y.-H. Cho, and Y. Park, "Subwavelength light focusing using random nanoparticles," *Nat Photonics*, vol. 7, pp. 455-459, 2013.

[4] I. M. Vellekoop, A. Legendijk, and A. P. Mosk, "Exploiting disorder for perfect focusing," *Nature Photonics*, vol. 4, pp. 320-322, 2010.

[5] Z. Yaqoob, D. Psaltis, M. S. Feld, and C. Yang, "Optical phase conjugation for turbidity suppression in biological samples," *Nature Photonics*, vol. 2, pp. 110-115, 2008.

[6] M. Cui and C. Yang, "Implementation of a digital optical phase conjugation system and its application to study the robustness of turbidity suppression by phase conjugation," *Optics Express*, vol. 18, pp. 3444-3455, 2010.

[7] Q. H. Liu, "Large-scale simulations of electromagnetic and acoustic measurements using the pseudospectral time-domain (PSTD) algorithm," *IEEE Transactions on Geoscience and Remote Sensing*, vol. 37, pp. 917-926, 1999.

[8] S. D. Gedney, "An anisotropic perfectly matched layer-absorbing medium for the truncation of FDTD lattices," *IEEE Transactions on Antennas and Propagation*, vol. 44, pp. 1630-1639, 1996.

[9] J. L. Hollmann, R. Horstmeyer, C. Yang, and C. A. DiMarzio, "Analysis and modeling of an ultrasound-modulated guide star to increase the depth of focusing in a turbid medium," J*ournal of Biomedical Optics*, vol. 18, 2013.

[10] A. Taflove and S. C. Hagness, *Computational Electrodynamics: The Finite-Difference Time-Domain Method*, Artech House, Boston, 2005.

[11] S. H. Tseng, "PSTD simulation of optical phase conjugation of light propagating long optical paths," *Optics Express*, vol. 17, pp. 5490-5495, 2009.

[12] T. W. Lee and S. C. Hagness, "A compact wave source condition for the pseudospectral time-domain method," *IEEE Wireless Propag. Lett.*, vol. 3, pp. 253-256, 2004.

[13] A. Taflove and S. C. Hagness, *Computational Electrodynamics: The Finite-Difference Time-Domain Method*, Artech House, 2000.

[14] S. H. Tseng, W. Ting, and S. Wang, "2-D PSTD Simulation of the time-reversed ultrasound-encoded deep-tissue imaging technique," *Biomedical Optics Express*, vol. 5, pp. 882-894, 2014.